



HAL
open science

Composite laminates reinforced by vertically aligned carbon nanotubes: Detailed manufacturing process, from nanotubes transfer to composite consolidation

Anh Tuan Le, Quentin Govignon, Samuel Rivallant, Thierry Cutard

► To cite this version:

Anh Tuan Le, Quentin Govignon, Samuel Rivallant, Thierry Cutard. Composite laminates reinforced by vertically aligned carbon nanotubes: Detailed manufacturing process, from nanotubes transfer to composite consolidation. *Journal of Composite Materials*, 2023, 57, pp.4239-4253. 10.1177/00219983231207441 . hal-04230095

HAL Id: hal-04230095

<https://imt-mines-albi.hal.science/hal-04230095>

Submitted on 11 Oct 2023

HAL is a multi-disciplinary open access archive for the deposit and dissemination of scientific research documents, whether they are published or not. The documents may come from teaching and research institutions in France or abroad, or from public or private research centers.

L'archive ouverte pluridisciplinaire **HAL**, est destinée au dépôt et à la diffusion de documents scientifiques de niveau recherche, publiés ou non, émanant des établissements d'enseignement et de recherche français ou étrangers, des laboratoires publics ou privés.

Composite laminates reinforced by vertically aligned carbon nanotubes: Detailed manufacturing process, from nanotubes transfer to composite consolidation

Anh Tuan Le^{1,2} , Quentin Govignon¹ , Samuel Rivallant²  and Thierry Cutard¹ 

Abstract

Nano-constituent incorporation into composites has been extensively studied in the literature due to its improvement in static and dynamic mechanical properties, as well as its prevention from interlaminar crack initiation and propagation. This work introduces a detailed manufacturing process of nano-engineered composite laminates, from impregnation to consolidation, without damaging the initial morphology of carbon nanotubes transferred on prepreg interfaces. Based on prepreg and vertically aligned carbon nanotubes (VACNTs) synthesized on an aluminium alloy (Al) substrate, the impregnation step allows for the transfer of VACNTs onto the prepreg surface through partial resin-rising capillarity. The Al alloy substrate is then removed from the VACNTs through a separation step, ensuring highly effective and repeatable transfer with more than 80% VACNTs transferred onto the prepreg surface. This paper provides insight into the impregnation and transfer processes and guides the choice of process parameters to ensure minimal VACNTs buckling during the consolidation of the hybrid composites at high pressure in an autoclave.

Introduction

Fibre reinforced polymer composites offer high in-plane mechanical performances, while out-of-plane properties require further investigation.^{1,2} To limit delamination of composites due to impact or through thickness solicitations, stitching of the reinforcement layers or Z-pinning have been proposed and provide good results, but the stitches and Z-pins provide discreet reinforcement, can damage the fibres, and may result in reduced in-plane properties.^{3,4} Introducing nano constituents within the resin or at the inter-layer has the opportunity to provide a more continuous through thickness reinforcement. In the literature, through-thickness incorporation of nano-constituents into composite layers, such as carbon nanotubes,^{5–12} graphene,^{13–18} nanosilica,^{19–23} has been suggested to improve mechanical properties.^{24–27} A few papers have discussed the addition of VACNTs at the inter-layer and their effect on the mechanical properties of the composites.^{28–33} With regard to static results, Garcia et al.²⁸ transfer VACNTs to the surface of

unidirectional prepreps. Crack opening tests in mode I for both the reference and nano-engineered composites were conducted. The results show an increase in toughness G_{Ic} from 36% (for AS4/8552 prepreg) to 43% (for IM7/977-3 prepreg) due to the introduction of VACNTs in the interplies. In the study of Veedu et al.,²⁹ CNTs are directly synthesized on SiC fuzzy fibres, the strong CNTs-fibres bonding explains the significant increase of 348% in mode I

¹Institut Clément ADER (ICA), Université de Toulouse, UMR CNRS 5312, IMT Mines Albi, INSA, ISAE-SUPAERO, UPS, Albi, France

²Institut Clément ADER (ICA), Université de Toulouse, UMR CNRS 5312, IMT Mines Albi, INSA, ISAE-SUPAERO, UPS, Toulouse, France

Corresponding author:

Quentin Govignon, Institut Clément ADER (ICA), Université de Toulouse, UMR CNRS, IMT Mines Albi, INSA, ISAE-SUPAERO, UPS, Campus Jarlard, Albi F-81013, France.
Email: quentin.govignon@mines-albi.fr

Data Availability Statement included at the end of the article

toughness and 54% in mode II toughness. Falzon et al.³⁰ observe a 31% increase of G_{Ic} for the T700/SE84LV composites with the presence of VACNTs, and 61% increase of G_{IIc} , for the T700/M21 nano-engineered composites. This improvement is explained by the VACNTs-resin adhesion observed on a microscopic scale. In terms of dynamic mechanical properties, Veedu et al.²⁹ have determined a damping ratio and a damping enhancement increase 669% and 514% respectively for nano-reinforced composites. Suhr et al.³² performed shear vibration tests on a 0.05 mm thick epoxy film reinforced with VACNTs, the presence of VACNTs contributes in the energy dissipation of the sample. A substantial difference is observed between the loss modulus of the reference samples (0.2–0.6 Hz) and that of the nano-reinforced samples (1.5–3.5 Hz). These significant changes in damping properties could be attributed to the friction properties between the VACNTs and the resin during the vibrational shear stress.

Many processes have been suggested to incorporate randomly oriented CNTs into composite matrices while reporting the risk of cluster formation and agglomeration on mechanical properties.^{34–40} As far as the authors know, few papers provide complete manufacturing instructions for nano-engineered composites that preserve the initial vertically aligned state of VACNTs, even though these composites seem most promising. In Garcia's thesis,⁴¹ the author suggests several resin-VACNTs incorporation methods: spin-coating, spraying gun, submersion, capillary rise. The impregnation of highly viscous resin into highly dense VACNTs forest by capillarity is found to be the most effective method. Beard et al.⁴² conducted a quantitative study of capillary rise, taking into account resin viscosity and resin-VACNTs impregnation time. Initially, epoxy resin, mixed with chromium components to create a contrast for EDS spectroscopy, is placed in a pool to observe resin capillary rise by SEM and X-ray tomography. Results show a partial and heterogeneous rise of resin in the VACNTs at different locations within the VACNTs forest. Boncel et al.⁴³ have also demonstrated the feasibility of partial resin capillary rise on polystyrene surface. In the current study, VACNTs forest is transferred directly onto prepreg surfaces, and the prepreg epoxy resin impregnates the VACNTs forest by capillarity to achieve partial impregnation. However, local coalescence of VACNTs due to resin-VACNTs surface tension is commonly observed. Sojoudi et al.⁴⁴ present totally impregnated VACNTs forest coalescing by surface tension, and this phenomenon is also observed in other studies.^{42,45} In the case of poorly controlled impregnation steps, VACNTs group in local zones, leaving some blank zones filled with resin, which could lead to delamination.

After impregnation, the VACNTs are lightly bonded to the prepreg, but need to be separated from their growth substrate before consolidation of a hybrid composite laminate. Dealing with the separation step, Wardle et al.⁴⁶ describe a separation

step using a metallic cylindrical roller. In this step, the prepreg is first bonded to a metal roller and the VACNTs-prepreg assembly is removed from the Si-based substrate so that the majority of VACNTs remains on prepreg surface. The quantitative values of the rotation speed and the pressure exerted on the cylinder are not reported, and the principle of the prepreg-VACNTs forest adhesion is not detailed. Using this method, the surface of nano-engineered prepreg is limited by the lateral surface of the cylinder. As an alternative method, Falzon et al.³⁰ propose impregnating the resin into VACNTs forest on the prepreg surface and then removing the VACNTs from their rigid Si-based substrate. The authors found that some areas of VACNTs remain on the substrate after separation. To optimise the transfer, the authors considered external parameters that can influence the transfer efficiency, such as pressure exerted on the transfer surface, impregnation temperature and impregnation time. In their study, the combination of 200 g of mass on a surface of $8 \times 25 \text{ mm}^2$ (equivalent to about 0.01 MPa of pressure) and heating at 90°C for 3 min gives the best transfer of VACNTs to the prepreg surface. The authors also found that a partial resin capillary rise in the VACNTs is more favourable than a complete resin capillary rise to ensure high transfer efficiency.

The SEM images in papers^{28,31} show that the morphology of VACNTs in the consolidated composites is altered, potentially due to high consolidation pressure (7 bar) or a low VACNTs density.

The purpose of this paper is to provide a detailed description of a manufacturing process for nano-engineered composites, which preserves the initial morphology of VACNTs after the consolidation. To achieve this objective, two steps have been followed.

In the transfer step, the VACNTs forests are transferred from their initial Al-based substrate to the prepreg surface. It is to note that the morphology of VACNTs transferred remains unchanged after the transfer step. The prepreg's resin impregnates the VACNTs forest through a controlled partial capillary rise of the resin. This approach exhibits high transfer efficiency at small and larger scales, and does not require other secondary techniques, such as functionalisation or sonication, to disperse the nanotubes within the composite matrix. By controlling process parameters, including temperature, pressure and heating time, the highly viscous polymeric resin can impregnate into the dense VACNTs forest without altering their initial morphology.

The nano-engineered composite samples were then consolidated in an autoclave. The high applied pressure during consolidation can cause VACNTs buckling. In this study, the optimal combination of autoclave parameters, such as pressure, temperature ramp and isothermal dwell durations is investigated to preserve the VACNTs morphology while ensuring high consolidation pressure and fibre content. The assessment of VACNTs morphology in

the consolidated resin is conducted through microscopic observations.

Experimental procedure

As the objective of the study is to create hybrid nano-engineered composite laminates using VACNTs at the interface between unidirectional carbon fibre preregs, the following two main steps have been proposed for the manufacturing process:

- VACNTs transfer from their aluminium alloy growth substrate onto the prepreg surface:
 - The impregnation involves bringing the VACNTs synthesized on Al-based substrate into contact with the prepreg surface, allowing the VACNTs forest to impregnate with resin from the prepreg by capillary rise;
 - The separation involves removing the Al-based substrate from the VACNTs, while the nanotubes remain bonded on the prepreg surface following the impregnation step.
- The consolidation step in an autoclave allows for full impregnation of the laminate with the available resin on the prepreg and subsequent resin crosslinking to consolidate the composite while attempting to preserve the VACNTs morphology as much as possible.

The following sections provide further details regarding the constituent materials and the consecutive steps involved in the process.

Materials

The prepreg used in this study is Hexply[®] M18/32%/UD116/M55J-6k/300 mm, which is a prepreg constituted of 116 g/m² of unidirectional M55J high modulus carbon fibres and 32% by weight of M18 resin, once consolidated ply thickness is about 125 μm. The resin viscosity is time

and temperature dependant. At 60°C, the initial resin viscosity is about 300 Pa.s.⁴⁷ The VACNTs in this study are multi-walled carbon nanotubes synthesized using Continuous Chemical Vapour Deposition (CCVD) method on a 50 μm thick flexible aluminium alloy (Al) substrate. A continuous VACNTs forest measuring 7 cm wide and 4 m long was synthesized and could be easily rolled up on a cylindrical support, as shown in Figure 1(a). The VACNTs have an average diameter of 8 nm, a density of about 2×10^{11} tubes/cm² and an average height of around 30 μm (Figure 1(b)).

For reference purposes, the end of the VACNTs forest attached to the growth substrate will be referred to as VACNTs' feet, and the canopy of the VACNTs forest will be referred to as VACNTs' heads. Due to the growth kinetics and density of nanotubes, the VACNTs' heads can be slightly less aligned and more disorganized compared to the VACNTs' feet. The pictograms shown in Figure 2 and affixed to all microscopic images (such as in Figure 1(b)) help to simplify the observations reading and understanding. The arrows represent the VACNTs in the feet-to-heads direction, the thick line represents the Al alloy substrate, and the grey disks represent the prepreg's carbon fibres.

Impregnation step

This step involves the impregnation of the resin from the prepreg into the VACNTs forest. The control of the capillary impregnation of viscous resin into the high density VACNTs synthesized on Al alloy substrate can be considered the most challenging aspect of this step.

Partial resin impregnation is focused on this study for these reasons:

- On microscopic scale, controlled resin impregnation can prevent VACNTs forest from coalescing due to surface tension during resin impregnation,^{41,44,48} preserving their initial morphology;

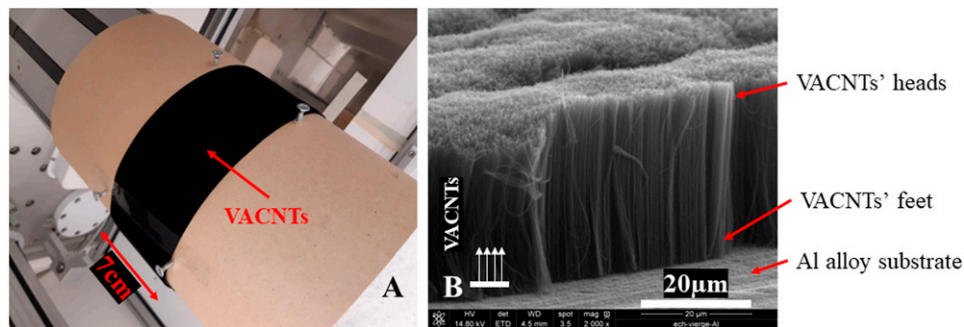


Figure 1. Vertically aligned carbon nanotubes (VACNTs) used for nano-engineered composite manufacturing: (a) VACNTs on deformable Al alloy substrate and (b) their initial morphology on microscopic scale.

- The absence of resin reaching the substrate (no additional bonding of VACNTs feet on the substrate) facilitates effective separation of the VACNTs from the substrate;
- Partial impregnation also allows the dry feet of VACNTs to be lightly pressed against the next layer of prepreg during consolidation and to penetrate the resin layer up to the prepreg's fibres;
- During consolidation step, each layer of VACNTs is brought into contact with another prepreg. Half of the resin rises into the VACNTs' feet from one ply, and the other half rises from the other ply, completing total impregnation of the resin in the VACNTs forests.

The feasibility of impregnating VACNTs forest with epoxy resin through capillary rise has been previously reported by the authors.⁴⁹ By changing the temperature and therefore the resin's viscosity, the impregnation of the VACNTs by the epoxy resin from the prepreg can be controlled. The resin viscosity and therefore the impregnation speed can be adjusted by changing the temperature during the process, as long as the resin crosslinking is kept to a minimum. To achieve this objective, the impregnation step is carried out under vacuum conditions, as shown in Figure 3. Three parameters are controlled in this process to ensure efficient impregnation: pressure exerted on the transfer surface, heating temperature and associated heating duration. A preliminary study was performed to estimate the values for these parameters. Pressures ranging from 0.2 to 2 bar were considered. High pressure can cause buckling of VACNTs during impregnation, resulting in non-aligned

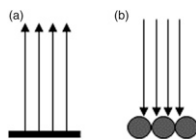


Figure 2. Pictograms defined and used to represent VACNTs on microscopic observation images with different types of support: (a) VACNTs on their initial Al alloy substrate; (b) VACNTs transferred onto prepreg surface. The feet and tips of the arrows respectively represent the feet and the head (the canopy of VACNTs forest) of the nanotubes.



Figure 3. Vacuum impregnation process: a piece of prepreg and an Al alloy growth substrate with the synthesised VACNTs placed on the prepreg' top are placed under a vacuum bag to distribute pressure evenly across the VACNTs-prepreg contact surface.

nanotubes after impregnation.⁴⁹ On the other hand, low pressure can reduce the contact between the VACNTs and the prepreg leading to local lack of transfer. Therefore, a vacuum pressure of 1 bar is selected for the impregnation process, as buckling was not observed at this pressure (see Figure 9). Initially, temperatures of 60°C and 80°C were tested for impregnation, but complete impregnation of resin in a very short time was observed at 80°C. Thus, the heating temperature was fixed at 60°C. Heating time varies from less than 5 min to 80 min. Microscopic observations were performed to determine the morphology of VACNTs and to confirm whether partial resin impregnation in VACNTs has been achieved (Figures 9 and 10).

Thus, the impregnation process involves several steps:

- Placing the prepreg on an aluminium plate;
- Positioning the VACNTs growth substrate on top with the VACNTs' heads towards the prepreg surface;
- Sealing the stack with a vacuum bag, and applying vacuum to create a contact pressure of 1 bar (0.1 MPa) as illustrated in Figure 3;
- In an oven previously heated to 60°C, placing the entire sample (aluminium plate + prepreg + VACNTs) on the top of a metal slab that was already pre-heated to provide thermal inertia and to speed up the temperature rise in the resin by conduction of the heat to the solid aluminium mould. The vacuum is maintained during heating;
- Removing the sample from the oven and accelerating the cooling down to room temperature through conduction by placing the sample on a cold metallic plate;
- Releasing the pressure, removing the sample from the aluminium mould, and storing it at -24°C to freeze the resin and prevent further impregnation as well as stopping any unwanted crosslinking of the resin before the separation and consolidation steps.

Separation step

The objective of the separation step is to detach the Al alloy substrate from the VACNTs, leaving the VACNTs on the prepreg surface, to create a nano-engineered semi-product. As mentioned in the previous section, partial resin capillary

rise is preferred to ensure efficient transfer during separation and the temperature must be controlled during separation. The deformability of Al alloy substrate enables the separation step to be carried out using a rolling steel cylinder, as illustrated in Figure 4.

In order to keep the resin in a solid or highly viscous state, to minimise resin flow, prevent cross-linking and ensure the cohesion of the VACNTs – prepreg interface, the temperature must be kept as low as possible. Concurrently, care must be ensured to avoid condensation on the material which could affect the resin polymerisation and adversely impact the composite mechanical properties. Based on the hygrothermal conditions of the laboratory, a constant temperature of 16°C was chosen for this study to remain above the dew point. A steel plate with a water-cooled circuit was used to provide a temperature-controlled surface for separation.

During the separation step, the sample is placed on the flat steel plate with the Al alloy substrate facing upwards, the prepreg surface was kept larger than the substrate surface in order to create a margin during separation and to avoid polluting the nano-transferred zone, as shown in Figure 4. To avoid any damage to the UD prepreg, the separation must always be carried out along the fibre direction. The prepreg was held in place on the surface by a double-sided tape that is bonded to one end of the prepreg, other mechanical means to hold in place the carbon fibre prepreps were also used for transfer on larger surfaces. At the same end, a piece of double-sided tape was placed on the edge of the aluminium alloy substrate, and a cylinder was rolled over the tape so that its adhesion to the substrate resulted in the gradual separation of the substrate from the VACNTs with a constant separation angle. This method

ensures that the local debonding conditions are uniform across the surface of the sample.

Consolidation process

To understand the effect of consolidation process parameters on the microscopic structure of VACNTs, three samples A, B and C were consolidated using different cure cycles. The consolidation pressure ranges from 1 bar in vacuum only process to 8 bar in an autoclave, the temperature ramp to the 180°C curing temperature was adapted with or without an intermediate step. Figure 5 provides details on the size and stacking sequence of these samples.

Figure 6 illustrates the evolution of process parameters during composite consolidation.

Observations from microscopic to macroscopic scale

Preparation for SEM observations. The purpose of microscopic observations on cross-sections of nano-transferred prepreg samples is to study the VACNTs morphology on the prepreg and to quantitatively determine the capillary-rise height of resin into VACNTs after different steps of the process. Non-consolidated samples were cut in the nano-transferred zone using a scalpel previously dipped in liquid nitrogen. Cutting with a cold scalpel prevents resin in the sample from smearing on the cutting plane. The samples were then fixed onto a holder after the separation process, and the observations were carried out using FEI-Novano SEM. Figure 7 illustrates one sample ready to be placed in the SEM. Figure 9 shows two examples of images of a section of nano-transferred prepreg.

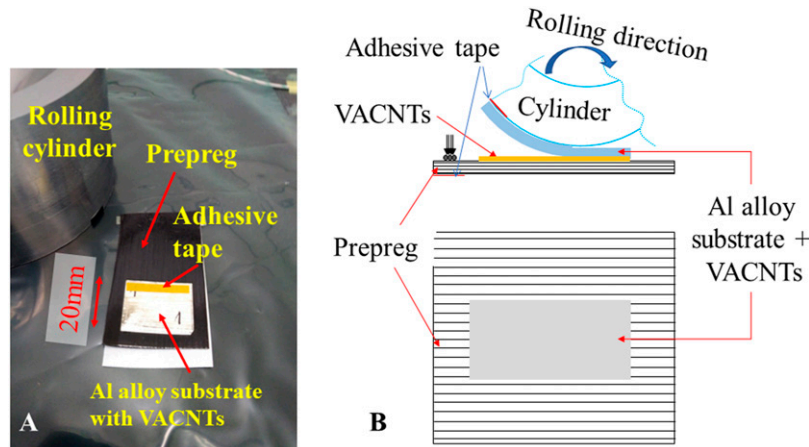


Figure 4. Separation process using metallic cylinder. The temperature of prepreg is maintained at 16°C using a temperature controlled plate placed beneath the sample, the fluid flow within the plate ensures that the temperature is maintained at a desired value.

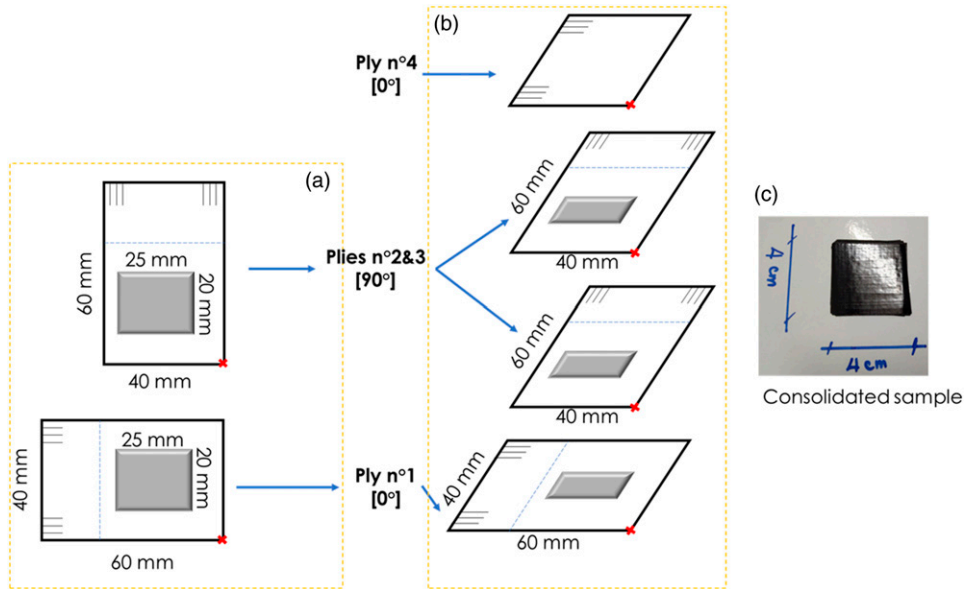


Figure 5. a) & b) 3 VACNTs forests ($25 \times 20 \text{ mm}^2$ areas) transferred between four prepreg plies in $[0^\circ, 90^\circ]_s$ stacking sequence. c) The sample is subsequently consolidated at high temperature to manufacture nano-engineered composites.

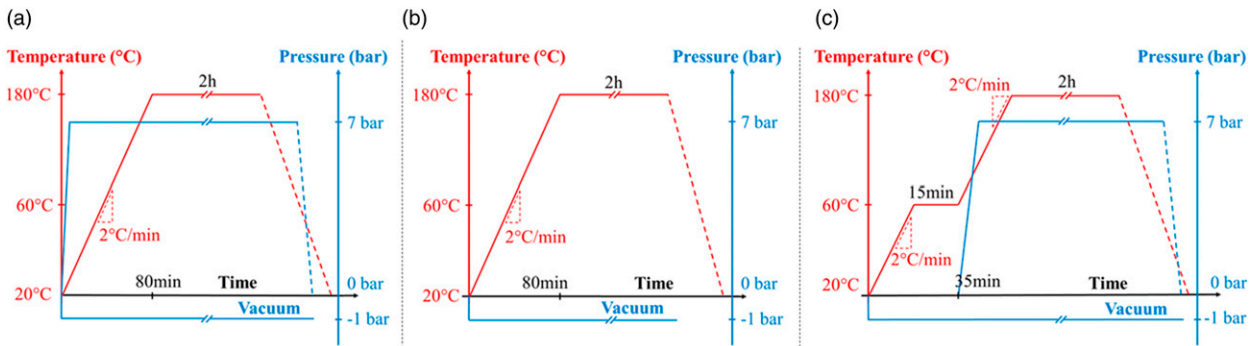


Figure 6. Evolutions of temperature and pressure during consolidation cycle of samples (a), (b) and (c).

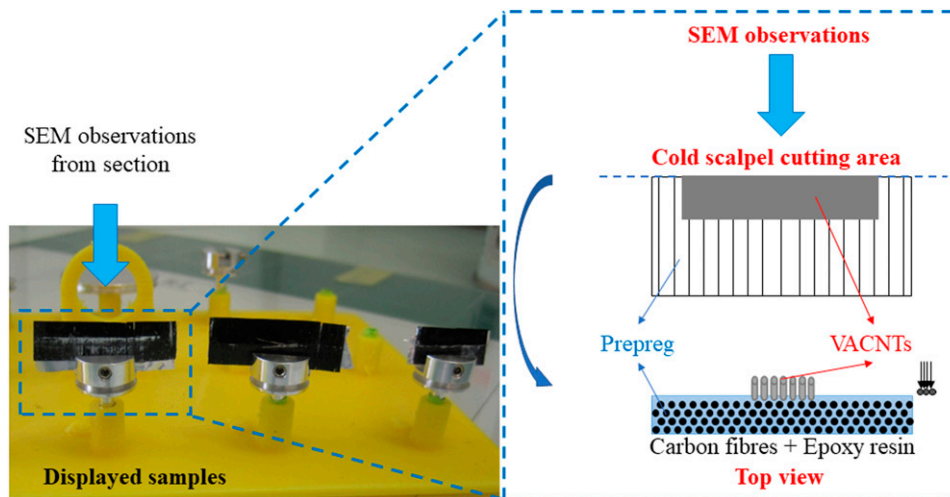


Figure 7. Positioning and orientation of samples for SEM observations of cross-sections after separation process.

Transfer rate determination. The surface of the Al alloy substrate before transfer and after separation as well as the prepreg after the separation step were photographed to determine the transfer efficiency of the VACNTs onto the prepreg surface. Images were then processed by an image analysis programme, which identifies the transferred and non-transferred areas based on a determined grey level thresholding.

Figure 8 illustrates three different samples of VACNTs: F2-30 μm , J2-33 μm and R2R-20 μm , where the bonding between VACNTs and their substrate can vary according to the growth conditions (F2, J2 and R2R references are linked to various growth conditions). All of them were transferred under the same conditions: 1 bar vacuum pressure and 60°C heating temperature for 10 min. As mentioned earlier, the separation step was carried out at a 16°C temperature.

In Figure 8, column A displays images of raw VACNTs substrates before impregnation. Column B displays images of VACNTs substrates after the separation step. Column C shows the prepreg surface covered by the VACNTs forest after transfer. By defining the threshold levels and finding common features between these three images A, B and C for each sample, the image analysis programme can overlay these images. Images in column D are the output from the programme with various coloured zones. The colour codes used to qualify these different zones are as follow:

- Black: absence of VACNTs on the initial substrate before impregnation;
- Cyan: presence of VACNTs on the prepreg only after impregnation (successful transfer);

- Magenta: presence of VACNTs on the Al alloy substrate only after impregnation (absence of transfer);
- Dark blue: areas with neither VACNTs covering on substrate nor prepreg surface. The presence of these areas is due to the loss of VACNTs during the transfer it can also signal a deviation in the positioning of the reference features during the superposition of the three images and call for a manual adjustment;
- White: presence of traces of VACNTs on both Al alloy substrate and prepreg. The transfer was only partially effective or VACNTs could be broken off during the separation process, their feet remaining bonded to the substrate.

The transfer rate is quantified as the ratio of the nano-transferred area after separation step measured in the images of column C (cyan and white areas in column D) to the initial area covered by VACNTs on the Al alloy substrate in images column A (all non-black areas in column D). The remaining rate is determined as the ratio of nano-covered area on Al alloy substrate after the separation as viewed in images column B (magenta and white areas in column D) to the initial area covered by VACNTs on the Al alloy substrate in images column A.

In Figure 8 column D, the white colour-coded areas are more prevalent in sample F2-30 μm compared to samples J2-33 μm and R2R-20 μm . This can be attributed to the presence of growth precursors and VACNTs' ends that remained attached to the surface of the substrate after separation. The presence of these broken VACNTs is

Substrates Reference	(a) VACNTs on Al substrate before transfer	(b) Al substrate after transfer	(c) Prepreg after transfer	(d) Image analysis results
F2-30 μm				
J2-33 μm				
R2R-20 μm				

Figure 8. Images considered to calculate the VACNTs transfer and remaining rates by an image analysis programme.

challenging for the calculation of transfer rate from images as the contrast between intact VACNTs and broken VACNTs is too low to distinguish them visually.

For J2-33 μm and R2R-20 μm recipes, the white and dark blue colour-coded areas are negligible, indicating the

absence of broken or lost VACNTs. The transfer rate, calculated from column C, and the remaining rate, determined from column B, add up to approximately 100%. With these recipes, it is therefore possible to calculate the transfer rate based on the remaining rate, and thus not

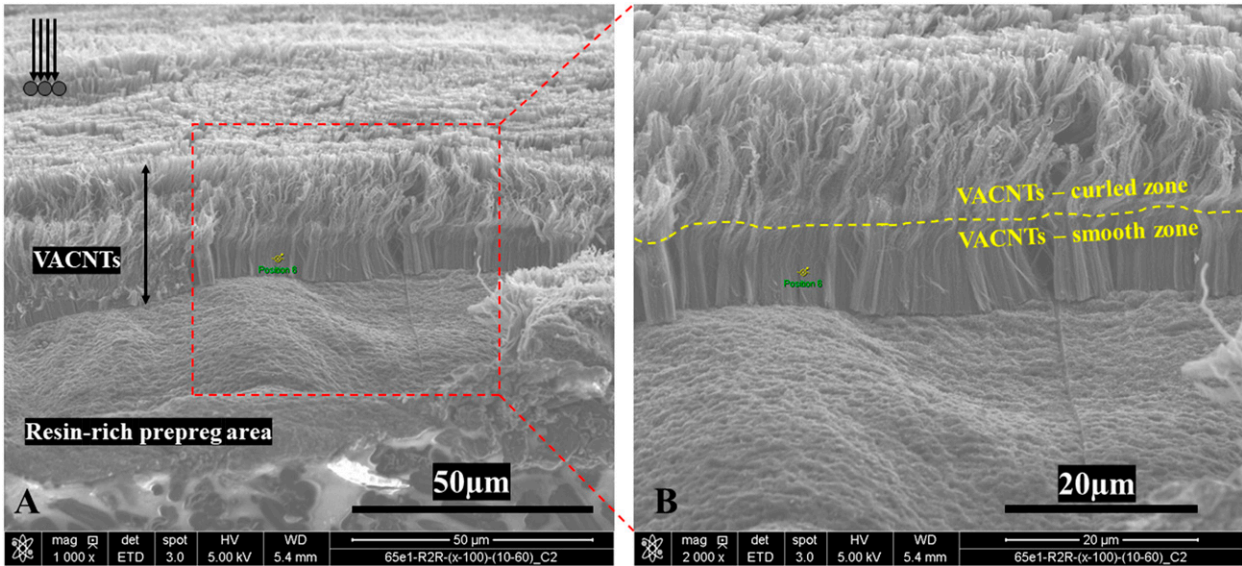


Figure 9. SEM images of partially impregnated VACNTs forest through a vacuum setting process (1 bar – 60°C – 10 min) after the separation step. The capillary rise height can be estimated by the grey shade, the slight coalescence zone and the VACNTs’ tortuosity. b) Yellow dotted line indicates the boundary between the VACNTs dry zone and the impregnated one.

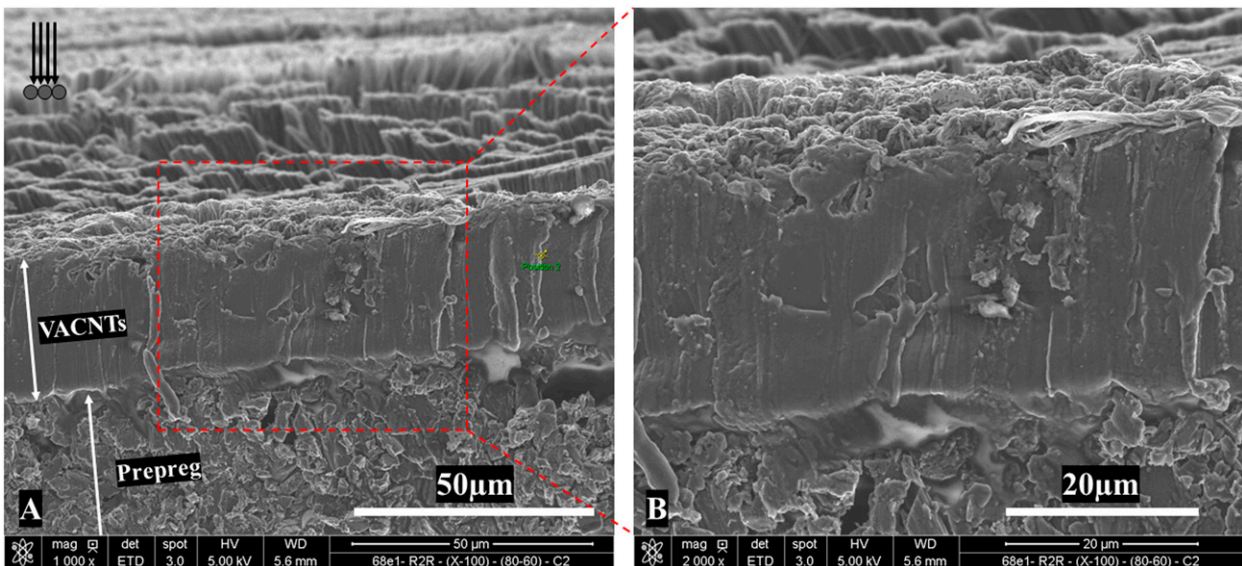


Figure 10. SEM images of totally impregnated VACNTs forest after the separation step. 80 min exposure under 60°C heating condition allow the resin to totally impregnate throughout the entire VACNTs forest.

require taking a picture of the prepreg after transfer. This can reduce the handling and possible contamination of the nano-engineered prepreg and should be preferred for production.

Table 1. Transfer rate measured in a feasibility study under varying impregnation conditions. Applied pressure 1 bar, sample size 25 * 25 mm².

Transfer conditions	Transfer rate (%)	Standard deviation (%)
2 min – 12°C (room temperature)	56.7	10.0
5 min – 60°C	81.5	1.1
10 min – 60°C	85.9	3.1
15 min – 60°C	84.5	4.3
20 min – 60°C	87.0	1.4

Table 2. Transfer rate measured during a composite manufacturing study with fixed processing conditions (1 bar pressure, 60°C, 10 min). Transfer rate calculated based on the remaining rate on the substrate.

N°	Transfer surface area	Remaining rate (%)	Transfer rate (%)
1		12.2	87.8
2	35 * 90 mm ²	22.1	77.9
3		21.5	78.5
4		18.8	81.2
5		35 * 150 mm ²	15.1
6	22.1		77.9
Mean			81.4
Standard deviation			4.2

Figure 8 demonstrates that the separation efficiency is recipe-dependent, with R2R–20 µm achieving a transfer efficiency of approximately 90%, as only a small amount of VACNTs remains on the Al alloy substrate thanks to a weak VACNTs to substrate adhesion.

Results and discussion

Partial resin impregnation into vertically aligned carbon nanotubes

The SEM images demonstrate the partial impregnation of resin into VACNTs forest through capillary rise under specific parameters (1 bar – 60°C – 10 min). The microscopic images in this section are taken after the separation process, before the samples are consolidated. Figure 9 shows that the VACNTs forest transferred onto prepreg surface maintain their initial morphology. The method to determine the level of capillary rise of the resin is detailed in a previous study⁴⁹, the yellow dotted line separates the wet and dry areas, indicating the limit between the resin-impregnated zones and the dry zones. The partial impregnation of resin into VACNTs forest is demonstrated under the impregnation process combination of 1 bar – 60°C – 10 min.

For a different impregnation condition of 1 bar –60°C –80 min, SEM images in Figure 10 illustrate that the VACNTs are completely impregnated by resin from the prepreg, indicating that this condition is unfavourable.

Under appropriate pressure and temperature conditions (1 bar - 60°C in this study), the control of the heating time enables partial capillary rise of the resin into the VACNTs

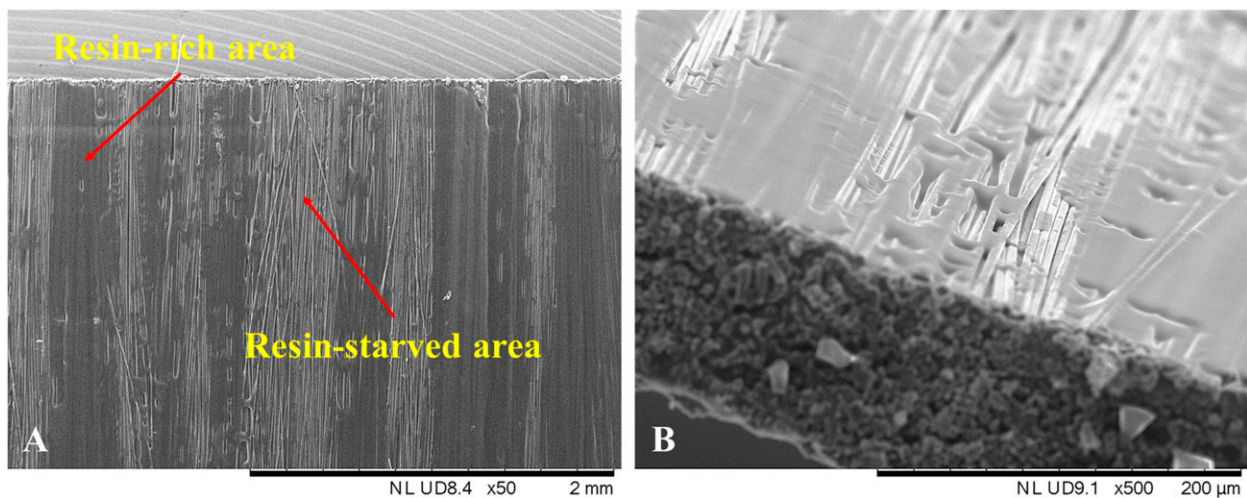


Figure 11. SEM observation of the Hexply M18/32%/UD116/M55J--K/300 mm prepreg showing alternance of resin rich and resin starved areas on the surface of the ply. a) top view ; b) cross section view.

forest, facilitating the bonding between the prepreg surface and the VACNTs' ends.

Separation process

In this study, the impact of heating time at 60°C – 1 bar on the transfer rate is established and presented in Table 1. As a balance between manufacturing time and transfer efficiency,

it was decided to employ a 10 min long isothermal dwell for the impregnation step. A longer impregnation period resulted in a slightly more elevated average transfer rate, but within the level of variability. Choosing a 20 min dwell time would require an additional 3 h to produce 20 layers for manufacturing a 2 mm thick composite. The results of the feasibility tests on a small scale indicate a transfer rate of almost 86% for a 10 min dwell, while the scalability tests on

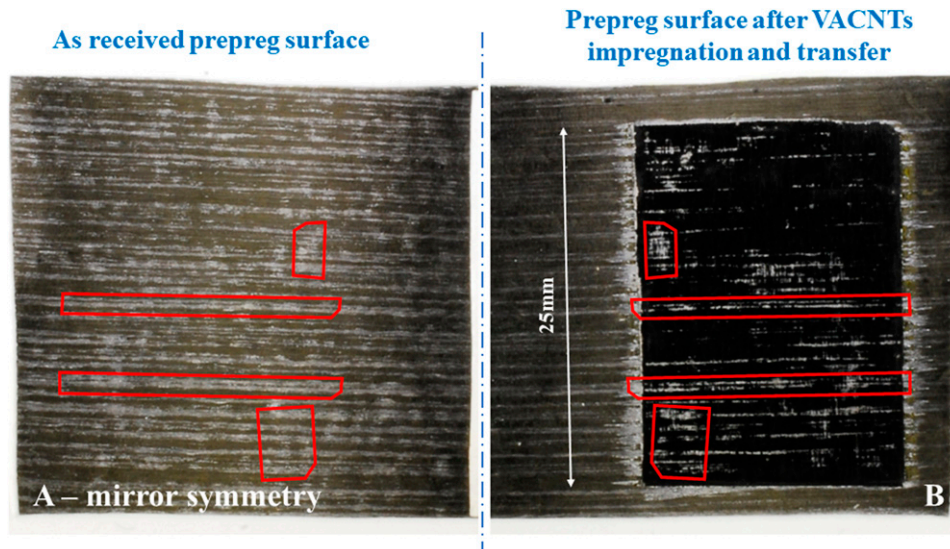


Figure 12. A piece of prepreg (top view): (a) as received, before VACNTs impregnation process and (b) after VACNTs impregnation and transfer. VACNTs are not totally transferred onto prepreg surface due to the lack of preimpregnated resin in some local prepreg zones (examples indicated in the red frames).

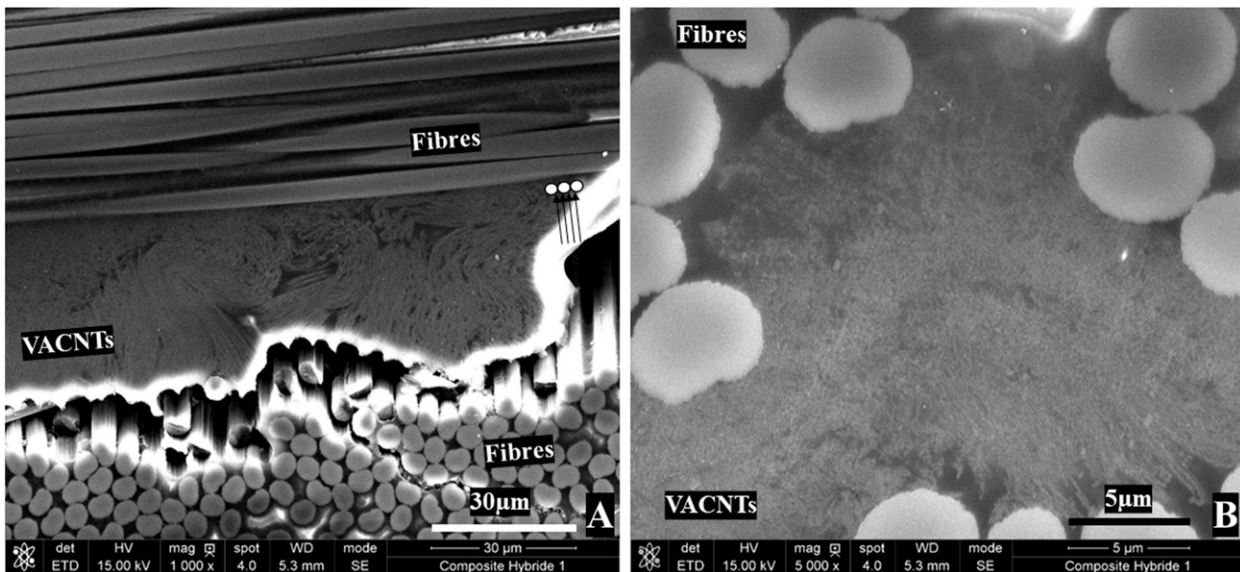


Figure 13. Cross-sectional SEM images (a) and (b) of sample A consolidated in an autoclave. Buckling of VACNTs is observed.

a larger scale show a transfer rate of 81%, demonstrating a high level of repeatability in the separation protocol with a high level of transfer rate, as shown in Table 2. 100% of transfer rate cannot be achieved in this study because the resin is not homogeneously distributed on the prepreg surface. Figure 11 presents SEM observation of the prepreg where resin rich and resin starved areas can be observed on the surface of the ply. This can also be seen at a macro-scale, in the left-hand picture of Figure 12 where resin starved areas appear in a lighter shade. Capillary impregnation and transfer will hence be more problematic in those areas, which is demonstrated looking at the red-framed areas where a lower transfer rate is

observed. After the transfer phase, the surface of the prepreg away from the VACNTs forest appears more regular, the combined action of heat and pressure may have permitted the resin to flow either through the thickness of the ply towards the surface or across from resin rich to resin starved areas. A clearer, resin starved area, can be observed surrounding the transferred VACNTs forest which corresponds to resin drawn into the VACNTs forest during the impregnation phase. It is therefore important for creating hybrid carbon-VACNTs composites, to ensure that the prepreg has enough excess resin and that this resin is homogeneously distributed across the surface.

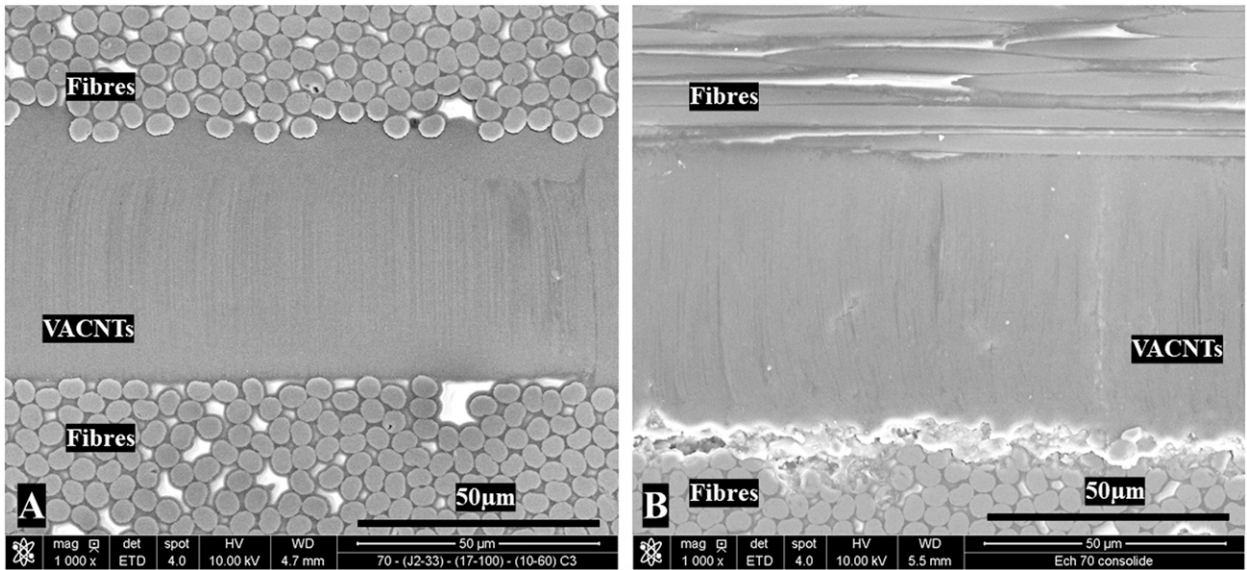


Figure 14. Cross-sectional SEM images (a) and (b) of sample B consolidated in an oven under vacuum pressure.

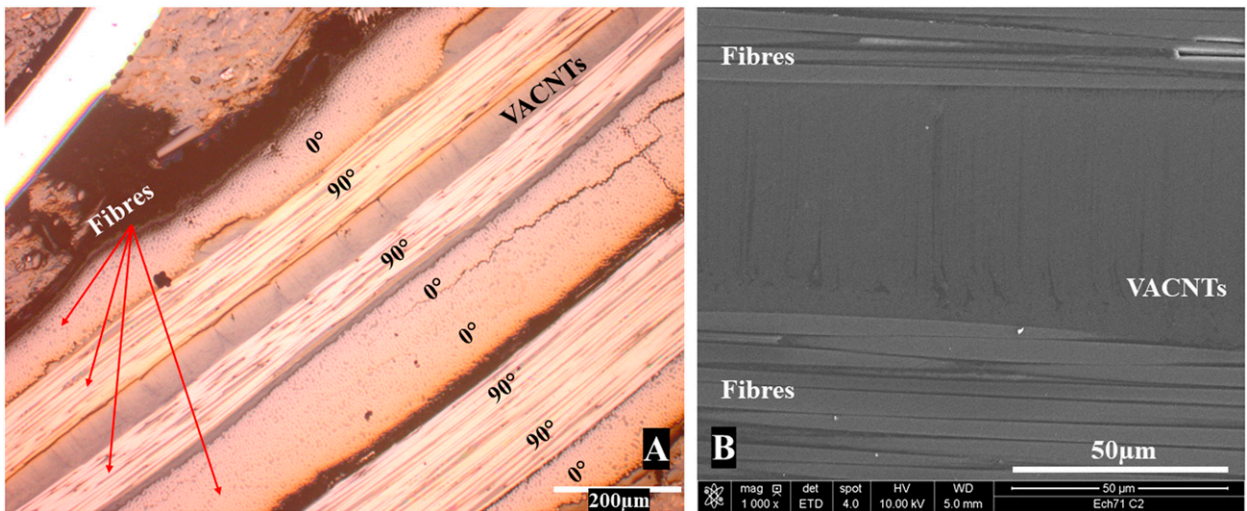


Figure 15. Cross-sectional optical microscopy (a) and SEM (b) images of sample C consolidated in an autoclave.

Consolidation process

In this section, the influence of consolidation parameters, such as pressure, heating temperature and associated heating duration, is investigated.

- The sample A shows that a pressure of 8 bar can cause buckling in the VACNTs forest (Figure 13);
- The sample B shows that a pressure of 1 bar does not damage the VACNTs morphology (Figure 14). However, the lower consolidation pressure can lead to residual porosity in the composite and to a low fibre volume fraction, which is not recommended by the supplier⁴⁷;
- The sample C takes into consideration results from the two previous samples to create an optimised process that respects the supplier's recommendations, without damaging the initial VACNTs' morphology (Figure 15). The first isothermal dwell at 60°C allows the resin to flow and fully impregnate the VACNTs before increasing the consolidation pressure. The higher compaction pressure of the second step is then distributed between the fibres and the resin, following Terzaghi's relation.⁵⁰ While the resin remains fluid, some can flow towards unfilled areas such as the breather cloth atop the laminate, and as the resin pressure decreases, the compaction applied on the VACNTs increases progressively. The presence of resin thus appears to help prevent the VACNTs from buckling under pressure. Overall, the parameter profile of sample C appears to provide the most favourable consolidation condition to maintain the alignment of the VACNTs while using a high consolidation pressure.

Conclusion

Due to the complexity of manufacturing nano-engineered composite materials, where the VACNTs in the forest must remain vertically aligned throughout the process, this paper provides a detailed step-by-step description of the manufacturing process from transferring VACNTs onto prepreg to the end of composite consolidation in an autoclave.

First, the choice of materials is paramount in order to successfully manufacture hybrid composites. The choice of prepreg material has to ensure a homogeneous resin distribution on the surface of the prepreg, and the resin flow needs to be sufficient to cover the resin needs calculated from the density and height of the VACNTs forest.

Vacuum transferring method is suggested in this study due to its advantages, including homogeneous pressure exertion on the nano-covered surface, controlled temperature distribution in an adjusted heating time and its

prevention of VACNTs from being exposed to exterior environment. Moreover, this method enables the impregnation of prepreg' viscous resin into extremely high-density VACNTs forest through capillary rise. The temperature and duration of the impregnation stage should be chosen based on the resin viscosity evolution to enable partial impregnation while preventing the resin to reach the growth substrate too quickly.

Al alloy substrate is separated from nano-transferred prepreg at a controlled temperature and with a constant peeling angle. The developed separation process ensures repeatable and effective VACNTs transfer rate of over 80%, and it was demonstrated that the transfer rate is highly dependent on the initial state of the prepreg and the resin repartition at its surface. Maintaining a sufficiently low temperature is necessary so that the resin remains in a jellified state and its cohesive force can overcome the adhesion of the VACNTs to their growth substrate.

Three samples have been consolidated to investigate the influence of autoclave cycle parameters (pressure, temperature level and duration of isothermal dwells) on VACNTs morphology after the autoclave cycle. SEM images illustrate VACNTs' buckling morphology at 8 bar consolidation pressure, while 1 bar of pressure is not recommended by the supplier during the consolidation stage. The autoclave cycle parameters for cure cycle C provide a compromise on these requirements, where a 60°C isothermal dwell with a 15 min duration, at 1 bar at the beginning of the autoclave cycle, allows the prepreg resin to impregnate into the VACNTs forest and helps prevent VACNTs from buckling under high pressure.

While the literature provides evidence of the potential improvement enabled by the introduction of a VACNTs inter-layer, the effect of the alignment and compression of the VACNTs layer hasn't yet been investigated. Providing means of controlling the morphology of the VACNTs forest during consolidation will enable a comparison of the effect of compression and buckling of the VACNTs on the mechanical response of the hybrid composites.

Acknowledgments

Several industrial partners were involved in this project: DynaS+, Thiot Ingenierie, CEA Saclay, CEA Cesta, NawaTechnologies, Armines and Airbus Defence & Space. The authors would like to acknowledge Alexandre Sangar (NawaTechnologies) for providing VACNTs substrates. Additionally, the authors would like to thank Karine Vieilleigne for the outstanding SEM images that inspired this study and contributed to the submission of this paper.

Declaration of conflicting interests

The author(s) declared no potential conflicts of interest with respect to the research, authorship, and/or publication of this article.

Funding

The author(s) disclosed receipt of the following financial support for the research, authorship, and/or publication of this article: This study was conducted as part of the FUI ATIHS project, which received funding from BPI France and Région Occitanie, the project's objective is to study the improvement of the strength of satellite structures against hypervelocity impacts caused by space debris.

Authorship contribution statement

Anh T Le: Writing - original draft, Investigation, Formal analysis, Visualisation, Data curation. Quentin Govignon: Writing - review & editing, Conceptualisation, Methodology, Visualisation, Data curation, Supervision. Samuel Rivallant: Writing - review & editing, Supervision. Thierry Cutard: Writing - review & editing, Supervision, Funding acquisition.

ORCID iDs

Anh T Le  <https://orcid.org/0000-0003-1596-5465>
 Quentin Govignon  <https://orcid.org/0000-0003-0971-0845>
 Samuel Rivallant  <https://orcid.org/0000-0002-8882-3161>
 Thierry Cutard  <https://orcid.org/0000-0003-1363-9957>

Data availability statement

The [datasets](#) generated and analysed during the current study are available from the corresponding author on reasonable request.

References

- Drake DA, Sullivan RW, Lovejoy AE, et al. Influence of stitching on the out-of-plane behavior of composite materials – a mechanistic review. *J Compos Mater* 2021; 55: 3307–3321. DOI: [10.1177/00219983211009290](https://doi.org/10.1177/00219983211009290).
- Thor M, Sause MGR and Hinterhölzl RM. Mechanisms of origin and classification of out-of-plane fiber waviness in composite materials—a review. *J Compos Sci* 2020; 4: 130. DOI: [10.3390/jcs4030130](https://doi.org/10.3390/jcs4030130).
- Song C, Fan W, Liu T, et al. A review on three-dimensional stitched composites and their research perspectives. *Compos Part Appl Sci Manuf* 2022; 153: 106730. DOI: [10.1016/j.compositesa.2021.106730](https://doi.org/10.1016/j.compositesa.2021.106730).
- Mouritz AP. Review of z-pinned composite laminates. *Compos Part Appl Sci Manuf* 2007; 38: 2383–2397. DOI: [10.1016/j.compositesa.2007.08.016](https://doi.org/10.1016/j.compositesa.2007.08.016).
- Xu N, Chen S, Li Y, et al. A hybrid 1D/2D coating strategy with MXene and CNT towards the interfacial reinforcement of carbon fiber/poly(ether ether ketone) composite. *Compos Part B Eng* 2022; 246: 110278. DOI: [10.1016/j.compositesb.2022.110278](https://doi.org/10.1016/j.compositesb.2022.110278).
- Imani Yengejeh S, Kazemi SA and Öchsner A. Carbon nanotubes as reinforcement in composites: a review of the analytical, numerical and experimental approaches. *Comput Mater Sci* 2017; 136: 85–101. DOI: [10.1016/j.commatsci.2017.04.023](https://doi.org/10.1016/j.commatsci.2017.04.023).
- Sun L, Warren GL, O'Reilly JY, et al. Mechanical properties of surface-functionalized SWCNT/epoxy composites. *Carbon* 2008; 46: 320–328. DOI: [10.1016/j.carbon.2007.11.051](https://doi.org/10.1016/j.carbon.2007.11.051).
- Hsieh TH, Kinloch AJ, Taylor AC, et al. The effect of silica nanoparticles and carbon nanotubes on the toughness of a thermosetting epoxy polymer. *J Appl Polym Sci* 2011; 119: 2135–2142. DOI: [10.1002/app.32937](https://doi.org/10.1002/app.32937).
- Gojny FH, Wichmann MHG, Köpke U, et al. Carbon nanotube-reinforced epoxy-composites: enhanced stiffness and fracture toughness at low nanotube content. *Compos Sci Technol* 2004; 64: 2363–2371. DOI: [10.1016/j.compscitech.2004.04.002](https://doi.org/10.1016/j.compscitech.2004.04.002).
- Gojny FH, Wichmann MHG, Fiedler B, et al. Influence of different carbon nanotubes on the mechanical properties of epoxy matrix composites – a comparative study. *Compos Sci Technol* 2005; 65: 2300–2313. DOI: [10.1016/j.compscitech.2005.04.021](https://doi.org/10.1016/j.compscitech.2005.04.021).
- Ayatollahi MR, Shadlou S and Shokrieh MM. Fracture toughness of epoxy/multi-walled carbon nanotube nanocomposites under bending and shear loading conditions. *Mater Des* 2011; 32: 2115–2124. DOI: [10.1016/j.matdes.2010.11.034](https://doi.org/10.1016/j.matdes.2010.11.034).
- Ayatollahi MR, Shadlou S and Shokrieh MM. Mixed mode brittle fracture in epoxy/multi-walled carbon nanotube nanocomposites. *Eng Fract Mech* 2011; 78: 2620–2632. DOI: [10.1016/j.engfracmech.2011.06.021](https://doi.org/10.1016/j.engfracmech.2011.06.021).
- Rafiee MA, Rafiee J, Wang Z, et al. Enhanced mechanical properties of nanocomposites at low graphene content. *ACS Nano* 2009; 3: 3884–3890. DOI: [10.1021/nn9010472](https://doi.org/10.1021/nn9010472).
- Stankovich S, Dikin DA, Dommett GHB, et al. Graphene-based composite materials. *Nature* 2006; 442: 282–286. DOI: [10.1038/nature04969](https://doi.org/10.1038/nature04969).
- Palermo V, Kinloch IA, Ligi S, et al. Nanoscale mechanics of graphene and graphene oxide in composites: a scientific and technological perspective. *Adv Mater* 2016; 28: 6232–6238. DOI: [10.1002/adma.201505469](https://doi.org/10.1002/adma.201505469).
- Salim MH, Kassab Z, Kassem I, et al. Hybrid nanocomposites based on graphene with cellulose nanocrystals/nanofibrils: from preparation to applications. In: Quaiss Ael K, Bouhfid R and Jawaid M (eds) *Graphene nanoparticles hybrid nanocomposites prep. Appl* Singapore: Springer, 2021, pp. 113–151. DOI: [10.1007/978-981-33-4988-9_4](https://doi.org/10.1007/978-981-33-4988-9_4).
- Xu Z and Gao C. In situ polymerization approach to graphene-reinforced nylon-6 composites. *Macromolecules* 2010; 43: 6716–6723. DOI: [10.1021/ma1009337](https://doi.org/10.1021/ma1009337).
- Zhao X, Zhang Q, Chen D, et al. Enhanced mechanical properties of graphene-based poly(vinyl alcohol) composites. *Macromolecules* 2010; 43: 2357–2363. DOI: [10.1021/ma902862u](https://doi.org/10.1021/ma902862u).
- Chen Y, Zhou S, Yang H, et al. Structure and properties of polyurethane/nanosilica composites. *J Appl Polym Sci* 2005; 95: 1032–1039. DOI: [10.1002/app.21180](https://doi.org/10.1002/app.21180).

20. Panaitescu DM, Vuluga Z, Radovici C, et al. Morphological investigation of PP/nanosilica composites containing SEBS. *Polym Test* 2012; 31: 355–365. DOI: [10.1016/j.polymertesting.2011.12.010](https://doi.org/10.1016/j.polymertesting.2011.12.010).
21. Nikje MMA and Tehrani ZM. Thermal and mechanical properties of polyurethane rigid foam/modified nanosilica composite. *Polym Eng Sci* 2010; 50: 468–473. DOI: [10.1002/pen.21559](https://doi.org/10.1002/pen.21559).
22. Saleh HM, El-Saied FA, Salaheldin TA, et al. Influence of severe climatic variability on the structural, mechanical and chemical stability of cement kiln dust-slag-nanosilica composite used for radwaste solidification. *Constr Build Mater* 2019; 218: 556–567. DOI: [10.1016/j.conbuildmat.2019.05.145](https://doi.org/10.1016/j.conbuildmat.2019.05.145).
23. Awad SA and Khalaf EM. Investigation of improvement of properties of polypropylene modified by nano silica composites. *Compos Commun* 2019; 12: 59–63. DOI: [10.1016/j.coco.2018.12.008](https://doi.org/10.1016/j.coco.2018.12.008).
24. Arash B, Wang Q and Varadan VK. Mechanical properties of carbon nanotube/polymer composites. *Sci Rep* 2014; 4: 6479. DOI: [10.1038/srep06479](https://doi.org/10.1038/srep06479).
25. Coleman JN, Khan U, Blau WJ, et al. Small but strong: a review of the mechanical properties of carbon nanotube–polymer composites. *Carbon* 2006; 44: 1624–1652. DOI: [10.1016/j.carbon.2006.02.038](https://doi.org/10.1016/j.carbon.2006.02.038).
26. Domun N, Hadavinia H, Zhang T, et al. Improving the fracture toughness and the strength of epoxy using nanomaterials – a review of the current status. *Nanoscale* 2015; 7: 10294–10329. DOI: [10.1039/C5NR01354B](https://doi.org/10.1039/C5NR01354B).
27. Sun X, Sun H, Li H, et al. Developing polymer composite materials: carbon nanotubes or graphene? *Adv Mater* 2013; 25: 5153–5176. DOI: [10.1002/adma.201301926](https://doi.org/10.1002/adma.201301926).
28. Garcia EJ, Wardle BL and John Hart A. Joining prepreg composite interfaces with aligned carbon nanotubes. *Compos Part Appl Sci Manuf* 2008; 39: 1065–1070. DOI: [10.1016/j.compositesa.2008.03.011](https://doi.org/10.1016/j.compositesa.2008.03.011).
29. Veedu VP, Cao A, Li X, et al. Multifunctional composites using reinforced laminae with carbon-nanotube forests. *Nat Mater* 2006; 5: 457–462. DOI: [10.1038/nmat1650](https://doi.org/10.1038/nmat1650).
30. Falzon BG, Hawkins SC, Huynh CP, et al. An investigation of mode I and mode II fracture toughness enhancement using aligned carbon nanotubes forests at the crack interface. *Compos Struct* 2013; 106: 65–73. DOI: [10.1016/j.compstruct.2013.05.051](https://doi.org/10.1016/j.compstruct.2013.05.051).
31. Ni X, Furtado C, Fritz NK, et al. Interlaminar to intralaminar mode I and II crack bifurcation due to aligned carbon nanotube reinforcement of aerospace-grade advanced composites. *Compos Sci Technol* 2020; 190: 108014. DOI: [10.1016/j.compscitech.2020.108014](https://doi.org/10.1016/j.compscitech.2020.108014).
32. Suhr J, Koratkar N, Keblinski P, et al. Viscoelasticity in carbon nanotube composites. *Nat Mater* 2005; 4: 134–137. DOI: [10.1038/nmat1293](https://doi.org/10.1038/nmat1293).
33. Le AT, Govignon Q, Rivallant S, et al. Mode I and mode II fracture behavior in nano-engineered long fiber reinforced composites. *Polym Compos* 2023; 44: 4016–4026. DOI: [10.1002/pc.27374](https://doi.org/10.1002/pc.27374).
34. Islam Rubel R, Hasan Ali M, Abu Jafor M, et al. Carbon nanotubes agglomeration in reinforced composites: a review. *AIMS Mater Sci* 2019; 6: 756–780. DOI: [10.3934/matersci.2019.5.756](https://doi.org/10.3934/matersci.2019.5.756).
35. Maghsoudlou MA, Barbaz Isfahani R, Saber-Samandari S, et al. Effect of interphase, curvature and agglomeration of SWCNTs on mechanical properties of polymer-based nanocomposites: experimental and numerical investigations. *Composites Part B* 2019; 175: 107119. DOI: [10.1016/j.compositesb.2019.107119](https://doi.org/10.1016/j.compositesb.2019.107119).
36. Inam F and Peijs T. Re-agglomeration of carbon nanotubes in two-part epoxy system; influence of the concentration. In: 5th International Bhurbhan Conference on Applied Science and Technology (IBCAST 2007), Islamabad, 8–11 January 2007, n. d.:8.
37. Smart SK, Ren WC, Cheng HM, et al. Shortened double-walled carbon nanotubes by high-energy ball milling. *Int J Nanotechnol* 2007; 4: 618–633. DOI: [10.1504/IJNT.2007.014756](https://doi.org/10.1504/IJNT.2007.014756).
38. Simões S, Viana F, Reis MAL, et al. Microstructural characterization of aluminum-carbon nanotube nanocomposites produced using different dispersion methods. *Microsc Microanal* 2016; 22: 725–732. DOI: [10.1017/S143192761600057X](https://doi.org/10.1017/S143192761600057X).
39. Shi D-L, Feng X-Q, Huang YY, et al. The effect of nanotube waviness and agglomeration on the elastic property of carbon nanotube-reinforced composites. *J Eng Mater Technol* 2004; 126: 250–257. DOI: [10.1115/1.1751182](https://doi.org/10.1115/1.1751182).
40. Alian AR, El-Borgi S and Meguid SA. Multiscale modeling of the effect of waviness and agglomeration of CNTs on the elastic properties of nanocomposites. *Comput Mater Sci* 2016; 117: 195–204. DOI: [10.1016/j.commatsci.2016.01.029](https://doi.org/10.1016/j.commatsci.2016.01.029).
41. García Enrique. *Characterization of composites with aligned carbon nanotubes (CNTs) as reinforcement*. Cambridge, MA: Massachusetts Institute of Technology, 2006.
42. Beard JD, Rouholamin D, Farmer BL, et al. Control and modelling of capillary flow of epoxy resin in aligned carbon nanotube forests. *RSC Adv* 2015; 5: 39433–39441. DOI: [10.1039/C5RA03393D](https://doi.org/10.1039/C5RA03393D).
43. Boncel S, Koziol KKK, Walczak KZ, et al. Infiltration of highly aligned carbon nanotube arrays with molten polystyrene. *Mater Lett* 2011; 65: 2299–2303. DOI: [10.1016/j.matlet.2011.04.065](https://doi.org/10.1016/j.matlet.2011.04.065).
44. Sojoudi H, Kim S, Zhao H, et al. Stable wettability control of nanoporous microstructures by iCVD coating of carbon nanotubes. *ACS Appl Mater Interfaces* 2017; 9: 43287–43299. DOI: [10.1021/acsami.7b13713](https://doi.org/10.1021/acsami.7b13713).
45. García EJ, Hart AJ, Wardle BL, et al. Fabrication of composite microstructures by capillarity-driven wetting of aligned carbon nanotubes with polymers. *Nanotechnology* 2007; 18: 165602. DOI: [10.1088/0957-4484/18/16/165602](https://doi.org/10.1088/0957-4484/18/16/165602).
46. Wardle BL, Hart AJ, Garcia EJ, et al. Nanostructure-reinforced composite articles and methods. *US8337979B2 Patent by Wardle Hart Garcia and Slocum*. 2012. <https://patents.google.com/patent/US8337979B2/en>.

47. Fiche technique des pré-imprégnés | Hexcel n.d. 2020. <https://www.hexcel.com/Resources/DataSheets/Prepreg> (accessed 1 July, 2020).
48. Kaur S, Sahoo S, Ajayan P, et al. Capillarity-driven assembly of carbon nanotubes on substrates into dense vertically aligned arrays. *Adv Mater* 2007; 19: 2984–2987. DOI: [10.1002/adma.200602883](https://doi.org/10.1002/adma.200602883).
49. Le AT, Govignon Q, Rivallant S, et al. Nano-engineered prepreg manufacturing: control of capillary rise of resin into VACNTs' forests. *Carbon Lett* 2023; 33: 1019–1025. DOI: [10.1007/s42823-023-00495-2](https://doi.org/10.1007/s42823-023-00495-2).
50. Terzaghi K. *Theoretical soil mechanics*. New York: John Wiley and Sons, 1943. DOI: [10.1002/9780470172766](https://doi.org/10.1002/9780470172766)